October, 1973

X-Ray Scattering from Gaseous 3He and 4He at Small Momentum Transfer

Robert Hallock, *University of Massachusetts - Amherst*

X-Ray Scattering from Gaseous ^{3}He and ^{4}He at Small Momentum Transfer*

Robert B. Hallock[†‡]

Department of Physics and Astronomy, University of Massachusetts, Amherst, Massachusetts 01002

(Received 19 January 1973; revised manuscript received 17 May 1973)

Several experiments are described in which the structure factor $S(k)$ was determined for gaseous ^{3}He and ^{4}He at temperatures near 5 K. In the momentum-transfer range $0.15 < k < 2.09$ Å^{-1} $S(k)$ was obtained for both ^{3}He and ^{4}He gas at densities of 1.95×10^{-3}, 2.66×10^{-3}, and 3.5×10^{-3} mole/cm^3. In the momentum-transfer range 0.133 Å$^{-1} < k < 1.125$ Å^{-1} $S(k)$ was obtained for ^{4}He gas at densities of 1.348×10^{-3}, 2.598×10^{-3}, 3.599×10^{-3}, and 5.557×10^{-3} mole/cm^3. For the ^{3}He temperature was 5.23 K while for the ^{4}He the temperature was 4.99 and 5.08 K. The first moment of the pair-correlation function was obtained by even-power-series fits to the structure-factor data at each density. Other power-series expansions have also been examined. The present experimental results are compared with $S(k)$ values obtained from modifications of the pair correlation function as calculated by Jordan and Fosdick for a temperature of 5 K.

I. INTRODUCTION

X-ray-scattering techniques provide powerful tools for the investigation of matter at the atomic level.[1] Commercial sources are available which provide x-ray wavelengths spanning the interatomic distances of normal materials. Thus, x-ray scattering can provide detailed information about the positions of atoms in matter. A measure of the positional correlation between atoms is the pair distribution function[2] $g(\vec{r})$. It is a conditional probability: it gives the chance of finding two atoms in the sample separated by the vector $\vec{r}$, normalized to unity at large separations. In the case of monatomic fluids—liquids and gases—it is a function of separation alone; i.e., $g(\vec{r}) = g(r)$. In a truly ideal gas all positions of one atom relative to another are equiprobable and hence for such a substance $g(r)$ is strictly unity for all particle separations.

The pair-correlation function is directly related to the observed intensity of scattering I, through a quantity known as the fluid structure factor S. The structure factor is related to $g(r)$ by a Fourier transform:

$$S(k) = 1 + \rho \int e^{i\vec{k}\cdot\vec{r}} [g(r) - 1]\, d^3r \,. \tag{1}$$

In Eq. (1) quantity k is the momentum transferred during the scattering event and is related to the observed angle of scattering θ through the well-known expression $k = (4\pi/\lambda)\sin\frac{1}{2}\theta$. ρ is the density, and λ the wavelength of the x ray. The observed intensity I is given in the usual manner[3] by

$$I = ANT(\sigma_e S + \sigma_i), \tag{2}$$

where A is the Thompson intensity, N the number of target atoms visible to both the source and the detector of x rays, and T is the transmission factor. σ_e is the coherent scattering factor (cross section) and σ_i is the incoherent scattering factor.

Experiments which seek to determine S for a given substance do so by comparison to a second substance. This is done so as to remove the necessity of calculating the number of atoms N, which can scatter x rays. We have chosen neon as our comparison substance since it is a nearly ideal gas (see Appendix A) at the temperature 77 K and pressures below 1 atm. Its use allows a determination of the structure factor S of the substance of interest. Let us rewrite Eq. (2) for neon:

$$I_N = AN_N T_N(\xi_e + \xi_i) \quad (S_N \simeq 1). \tag{3}$$

Forming the ratio equation (2)/equation (3), we have

$$S = \frac{I T_N \rho_N}{I_N T \rho} \frac{\xi_e + \xi_i}{\sigma_e} - \frac{\sigma_i}{\sigma_e} \,. \tag{4}$$

In this manner the ratio of numbers of atoms is replaced by the ratio of number densities which is readily calculated. Equation (4) will be used extensively to extract the structure factors of interest from the measured intensities.

The present work was motivated by the work of Achter and Meyer[4] who found, as I did,[5] independently, that considerable structure is present in helium gas at temperatures near 5 K and pressures near 1 atm. Gordon[6] has indicated that a suggestion of this structure in helium gas was present in the early work of Gordon, Shaw, and Daunt.[7] In this work we have studied $S(k)$ for both ^{3}He and ^{4}He gas at several pressures and temperatures near 5 K. In several cases the number densities were matched so that a more direct comparison between the two gases could be made. These measurements were limited to values of the momentum transfer below 2.1 Å^{-1} owing to constraints in

the x-ray spectrometer.[8]

Section II contains a discussion of the structure factor of a fluid at finite temperatures, and includes a brief description of the theory which we compare to our work. Section III contains comments relative to the apparatus. The final sections contain comments on the analysis of the data, the errors encountered, and a general discussion of the structure factors and the moments of the correlation function. The appendices contain discussions of departures from ideality of the gases we have studied as well as tables of structure factor values resulting from this study.

II. STRUCTURE FACTOR OF PERFECT AND IMPERFECT FLUIDS

As we have already indicated, the perfect or ideal fluid is one in which all positions of one atom relative to any other occur with equal probability. Since $g(r)=1$ for such a case, the structure factor for an ideal fluid is strictly unity for all values of the momentum transfer. In a real fluid this condition is approached in the low-density limit. Goldstein[9] has pointed out that for a real fluid at any finite temperature the structure factor can be expressed as

$$S(k)=\rho_0 k_B T X_T+\sum_{n=1}^{\infty}(-1)^n k^{2n} r_G^{(2n)}[(2n+1)!]^{-1}. \tag{5}$$

Here ρ_0 is the density, k_B is the Boltzmann constant, T is the temperature, X_T is the isothermal compressibility, k is the momentum transfer, and $r_G^{(2n)}$ is the $2n$th moment of the pair-correlation function defined by

$$r_G^{(2n)}=4\pi\rho_0\int r^{2n}[g(r)-1]r^2\,dr. \tag{6}$$

Again we point out that we have taken $g(r)\to 1$ as $r\to\infty$. Note that this choice agrees with that used by some authors (e.g., Jordan and Fosdick[10] and Massey[11]) but differs with that used by others (e.g., Goldstein[9]). This expression is consistent with the statement that $S(k)=1$ for all values of the momentum transfer in the case of an ideal gas because for that case $r_G^{(2n)}=0$ for all values of n and $X_T=(\rho_0 k_B T)^{-1}$ as can be readily seen from the ideal-gas law. In principle it is possible to obtain the moments $r_G^{(2n)}$ by even power series fits to the structure-factor data.

Few calculations of the structure factor at low density have been carried out. Most authors[12] have focused attention on the difficult problem of obtaining the pair-correlation function and hence the detailed properties of liquids. There have, however, been a few notable exceptions. As in the case of liquids, calculations for the gas proceed by means of the pair-correlation function. Larsen, Witte, and Kilpatrick[13] were led to a quantum mechanical investigation of the pair-

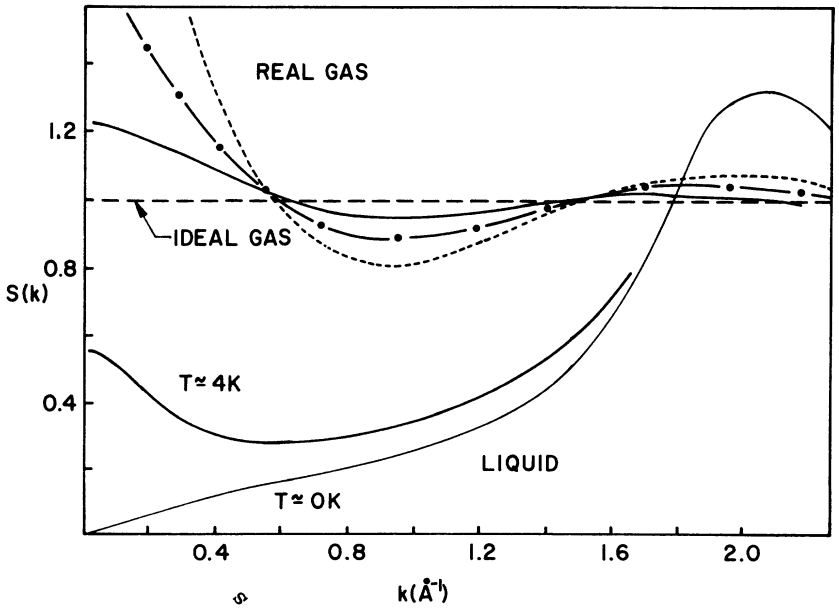

FIG. 1. Typical structure factors to be expected for the quantum gases and liquids. As indicated in the text, an ideal gas (long-dashed line) has a structure factor of unity for all values of the momentum transfer. The curves represent the structure factor for gaseous and liquid helium. Dilute (solid line) helium gas shows less structure than dense (short-dashed line) gas. Two typical curves for liquid helium are also shown. In all cases the intercept $S(0)$ can be found from $S(0)=\rho_0 k_B T X_T$. The peaking in the region of 2 Å^{-1} results from the maximum in the pair-correlation function associated with the equilibrium interatomic distance.

correlation function of ^{4}He gas at low temperatures by their interest in the role of statistics in the second virial coefficient and the general equation of state. Starting with the quantum-mechanical expression for the joint probability,[14] these workers expressed the density-independent part of the quantum-mechanical pair-correlation function as a sum over states symmetric under particle interchange. Following Lee and Yang[15] they partitioned the sum into two parts: one subject to Boltzmann statistics (which was called the direct term); the other (which was called the exchange term) subject to quantum statistics. These sums were then accomplished using Runge-Kutta[16] techniques to integrate the Schrödinger equation and hence obtain the wave functions. The results of their work suggested that for temperatures in excess of about 2 K the contribution to the pair correlation function due to the effects of quantum statistics was quite small.

Fosdick and Jordan,[17] by a very different technique, have carried out a similar calculation. These workers used the Wiener integral formulation[18] of the summation involved in the quantum mechanical pair-correlation function. The integrals encountered in their work were evaluated by Monte Carlo techniques. Their work also involved a separation of the contribution to the correlation function into a direct and an exchange term. While the published results of Larsen *et al.*[13] are restricted to $T \leq 2$ K, the results of Fosdick and Jordan[17] are given for $T \geq 2$ K. Jordan and Fosdick[10] later extended their work (using the same techniques) so as to include three particle effects on the pair-correlation function. They found that for temperatures below about 5 K, these three particle effects were not significant. Since the theoretical effort of these workers overlaps our experiments, we shall have occasion to compare our work with their predictions in a later section.

The type of results one expects when studying structure factors can be seen by reference to the schematic drawing (Fig. 1). In all cases, as can be seen from Eq. (5), the structure factor in the limit $k \to 0$ is given by $S(0) = \rho_0 k_B T \chi_T$. Thus, at the critical point for the fluid in question the structure factor diverges as the compressibility in the low-momentum transfer limit. In the low-density limit, the structure factor approaches the ideal-gas behavior characterized by unity for all values of the momentum transfer. This figure is drawn for helium so that in the limit of a cold liquid,

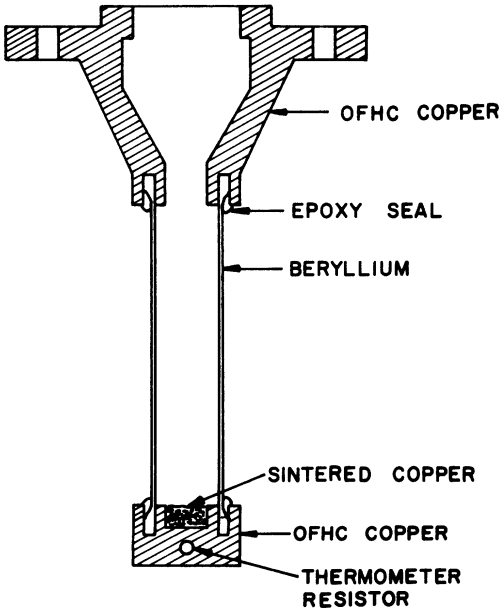

FIG. 2. Beryllium target cell. The beryllium shell has a wall thickness of 0.010 in. over its entire length. The upper and lower sections are made from OFHC copper. The beryllium is bonded to the copper with epoxy.

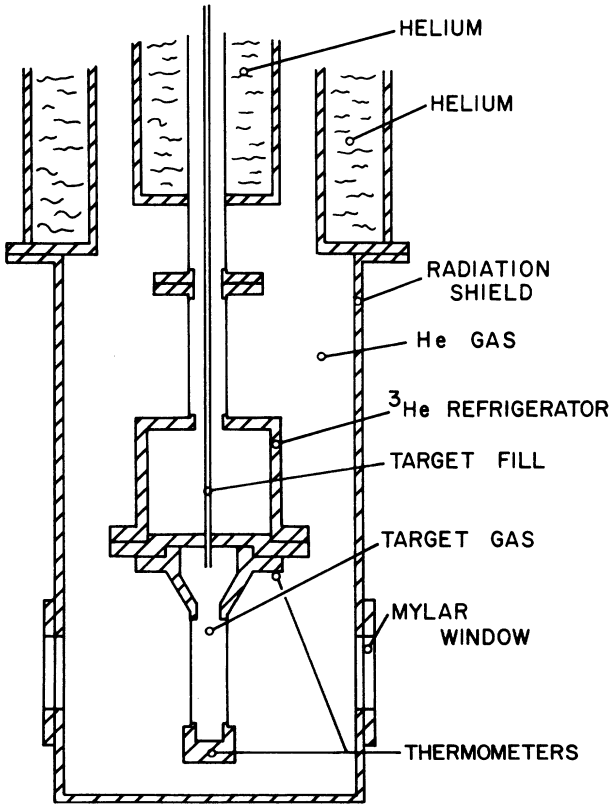

FIG. 3. General low-temperature apparatus. Helium gas at a pressure of 5×10^{-3} Torr is used to provide thermal contact between the target and the thermal radiation shield, the equilibrium temperature at the target is typically near 5 K. The ^{3}He refrigerator was used for support only.

$S(0)=0$. Experiments at a variety of temperatures in the liquid and gas phases can be expected to show a smooth transition from one region of the figure to the next. As we shall see later the results of this work follow expectations in this regard.

III. APPARATUS AND EXPERIMENTAL TECHNIQUE

The cryogenic apparatus used for this work is the same as that used in our earlier work[19,20] on liquid ^{4}He and liquid ^{3}He. The basic x-ray spectrometer is also identical. Aside from comments concerning the target cell and the maintenance of temperatures near 5 K, no further comments regarding the apparatus are necessary. The reader is referred to Ref. 19 for pertinent details.

Since we were working at a variety of pressures up to about 2 atm, the Mylar[21] target cells used in some of our earlier work were discarded in favor of a more rigid beryllium cell of the type shown in Fig. 2. The target cell was attached directly to the (unused) ^{3}He refrigerator (see Fig. 3) for support.

Temperatures were maintained at $T=5$ K by the introduction of 5×10^{-3} Torr of helium gas in the space surrounding the target cell. Since the thermal radiation shield (see Fig. 3) which was in intimate contact with the main helium bath was provided with 0.001-in.-thick windows made from aluminized Mylar, the helium gas was confined to the region between the target and the radiation shield.

The gas in the target cell was cooled by conduction through contact with the beryllium and copper walls of the target cell. A sintered copper sponge in the base of the target cell improved the surface area available for contact. Thermometry was accomplished by carbon resistors used in an ac Wheatstone-bridge circuit. The resistors were calibrated in a separate apparatus by comparing them to a calibrated germanium-resistance thermometer.[22] To facilitate the comparison and hence the calibration of the carbon thermometers the following precautions were taken: an oxygen-free high-conductivity (OFHC) copper block was prepared and the resistors and the germanium thermometers were inserted into holes drilled into the block. Apiezon[23] *N* grease was used to fix the resistors and germanium thermometer in place. The copper block was then mounted on a probe and lowered into the helium space of a separate Dewar which could be pressurized to 3 atm. After equilibrium was reached at each pressure (a heater at the bottom of the helium bath aided in attaining equilibrium) the resistors were calibrated by comparison to the calibrated germanium thermometer. The same ac techniques were used on the carbon resistors for both the calibration and later temperature measurement. Prior to calibration the carbon resistors had been cycled to helium temperatures three times.

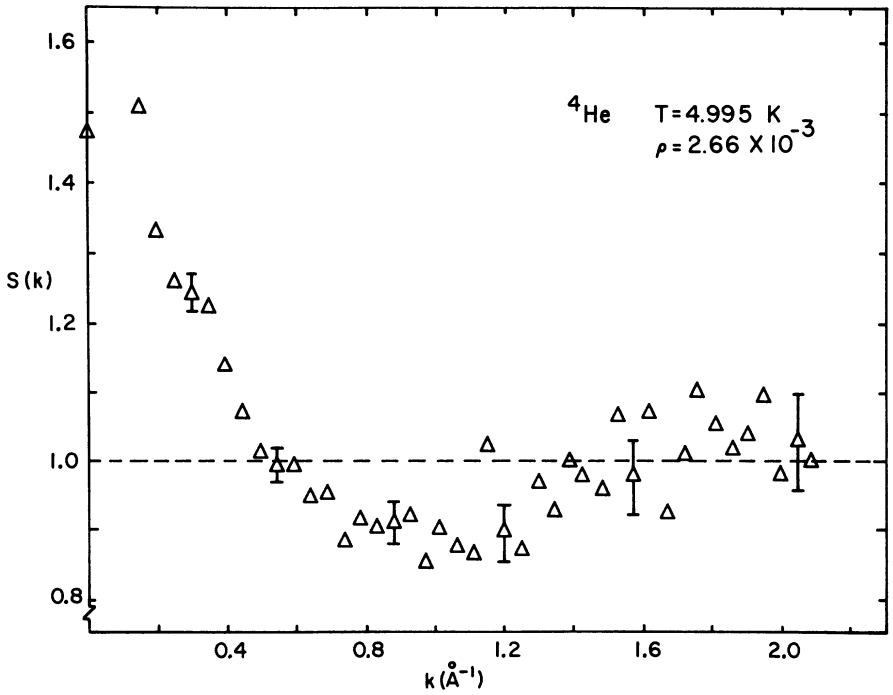

FIG. 4. Structure-factor data typical of that found in these measurements. The error bars are representative of a one standard-deviation error due to counting statistics alone. The triangle on the ordinate is the intercept calculated from the virial equation. The density units are mole/cm^3.

Since the heat load on the radiation shield pictured in Fig. 3 remained essentially constant during a given run, the presence of the low-pressure gas in the region between the target and the radiation shield ensured that the temperature of the target cell remained constant to within a few mK for any given target gas without the need for electronic temperature regulation. In view of the rather large statistical errors expected[24] in the scattering data, no attempt was made to improve on this temperature stability.

Although detailed comments regarding the spectrometer and data-collection scheme have been relegated to the references, a few points regarding the resolution and spectral purity of the x-ray beam should be repeated. The primary x-ray beam was derived from the line source of a General Electric CA-7*H* copper tube which was both voltage regulated and current stabilized. Fluctuations in main beam intensity amounted to less than 2%. The vertical and horizontal divergence of the beam was limited by slits and the measured over-all angular resolution was found to be about 0.55 deg. The CuK beam was purified by a nickel filter placed at the detector. It served to reduce the initial 12% admixture of K_β so that the final beam was at least 99% K_α. The counter[25] (sealed xenon-methane) was of sufficient resolution (about 1 KeV) to allow computer resolution of the initial impure beam into K_α and K_β components.

The system gain was checked before and after each sweep through the scattering angles of interest. These checks as well as a monitoring of room background levels indicated no significant changes in system gain or background during the various experiments.

IV. DATA COLLECTION, ANALYSIS, AND COMMENTS CONCERNING ERRORS

As has already been indicated, the structure factor of interest is determined from the observed intensities by means of the expression

$$S = \frac{I T_N \rho_N}{I_N T \rho} \frac{\xi_e + \xi_i}{\sigma_e} - \frac{\sigma_i}{\sigma_e} . \tag{4}$$

In an actual experiment the quantities denoted I and I_N are the scattering intensities observed in scattering from helium gas and the neon-normalization gas alone. To obtain these numbers as a function of angle a typical run always must consist of several sweeps to obtain scattering from the empty target cell. Typically, data were taken for several thousand counts at each angle and the sweeps of about 30 angles were always repeated at least once to check reproducibility and improve the statistics. It is to be emphasized that after each gas sample (^{3}He, ^{4}He, or neon) was used as a target, the background from the empty cell was taken again. Also, data for a given sample were always taken at the highest pressure first so that in the unlikely event that contamination should form on the inside of the target cell it would be a

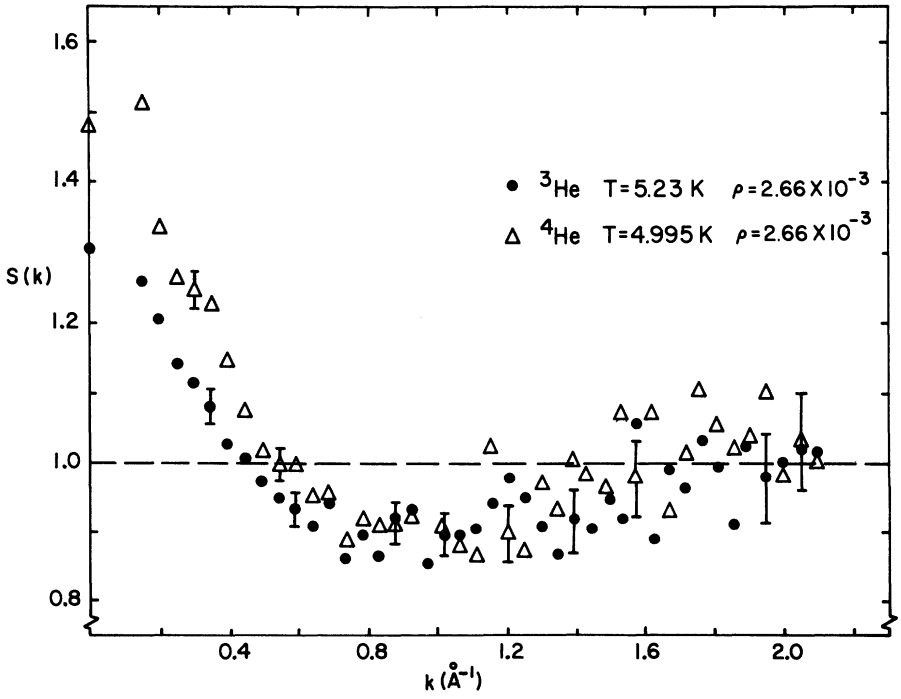

FIG. 5. Comparison of ^{3}He and ^{4}He at the same number density $\rho = 2.66 \times 10^{-3}$ mole/cm^3. As indicated in the figure the two measurements were taken at slightly different temperatures and hence the comparison is not perfect.

constant for all runs with the given substance. As a precaution to guard against the possibility of contamination the target gases were all filtered twice at liquid-nitrogen temperature by passing them through activated charcoal. As an additional precaution the helium samples were passed through a trap at 4.2 K.

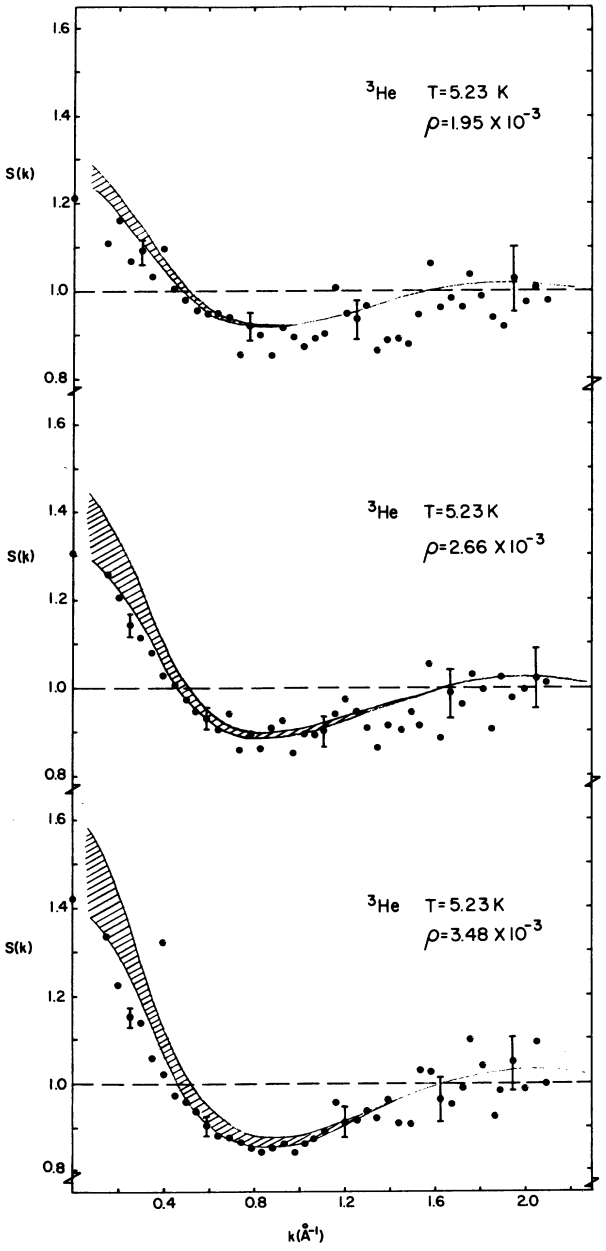

FIG. 6. Structure-factor values for ^{3}He as a function of momentum transfer. The solid band represents the theoretical structure factor obtained from the pair-correlation function study by Jordan and Fosdick. As explained in detail in the text, the spreading of theoretical values results from uncertainties in extending the correlation functions of Jordan and Fosdick to large enough r values to allow a reasonable Fourier transformation. The densities are given in mole/cm^3.

The statistical errors due to counting which we have encountered in this work are larger than those generally found when investigating *liquid* helium. The reason is simply that the low densities involved give rise to less scattering centers per cm^3 when investigating gaseous samples. This low density compounds the difficulty of dealing with helium, i.e., the presence of only two electrons per atom. At small values of the momentum transfer the structure factor for the gas is the order of unity as compared with 0.1 for the liquid. The largest errors relative to the liquid case are thus encountered in the range $k \gtrsim 2$ Å^{-1}, where the structure factors are comparable (but, of course, the densities are not).

As is usual in experiments of this type a variety of systematic errors are possible. Since the helium is dilute we have taken its transmission factor to be unity. Again, owing to the dilute nature of the sample, we expect that multiple-scattering effects[26] amount to substantially less than 1% and hence have neglected them. Some multiple-scattering effects are expected in the case of neon and we estimate that the over-all effect of neglecting these may introduce an error of 1% or so. The question of the departure from ideality of the neon is considered in detail in Appendix A. This problem is expected to contribute a maximum error of 1%. We expect that our total systematic error is 2–3%. Random errors were also encountered. Over the course of these measurements the x-ray beam was observed to be stable to about 2%. Counting statistics were generally between 2 and 7% with the larger error coming at the larger angles. Our total error then is expected to be on the order of 4–9% depending on the scattering angle (see tables in Appendix B). The data has been analyzed by inserting the measured intensities (corrected for empty target scattering) directly into Eq. (4). The scattering factors for helium[27] and neon[28] were taken from published values as were the transmission coefficients.[29] The densities were taken from the Berlin[30] virial equation in the case of neon and from Keller[31] in the case of ^{3}He and ^{4}He. As we have previously mentioned, neon[5] was chosen as the normalization gas for the work reported here since it is nearly ideal at the pressures ($\simeq 1$ atm) and temperatures ($\simeq 77$ K) used.

V. RESULTS AND DISCUSSION

Results representative of those we have found are shown in the figures. Typical error bars are shown on each figure. In all cases the error bars

represent plus- and minus-one standard deviation *due to counting statistics alone*. The symbol plotted on the $S(k)$ axis for $k=0$ is determined from $S(0)=\rho_0 k_B T X_T$ in the manner detailed in Appendix A. In all cases, reference to the figures indicates that our data are consistent with the expected intercept.

Figure 4 is typical of the results we have obtained. As we have previously indicated our errors are largest at the largest values of the momentum transfer. Figure 5 displays these same results for ^{4}He along with results for ^{3}He taken at the same number density. Again, the intercepts are obtained from the compressibility through use of the virial coefficients. Note that the temperatures for the measurements on these two gases were not quite the same.

In Figs. 6 and 7 we compare our results for ^{3}He (Fig. 6) and ^{4}He (Fig. 7) in the momentum transfer range $0.15\ \text{Å}^{-1} < k < 2.09\ \text{Å}^{-1}$ with calculated curves for the structure factor at the experimental densities. These structure-factor curves were obtained from the work of Jordan and Fosdick[10] by a procedure which we now explain.

The work of Jordan and Fosdick[10] was, as we have previously indicated, a quantum-mechanical calculation of the pair-correlation function. Their results are presented in the form

$$g(r)=W_2(r)[1+\rho g_1(r)]\,, \tag{7}$$

where $W_2(r)$ is the correlation function given by Fosdick and Jordan[17] considering particle pairs alone and $g_1(r)$ is a correction obtained by considering three particle effects. Tables of values for $W_2(r)$ and $g_1(r)$ are available[32] at several values of the temperature from 5 to 273 K. Since our experiments were carried out in the vicinity of 5 K, we have compared the theory at 5 K to our results. At 5 K, the table of values for $W_2(r)$ and $g_1(r)$ is limited due[32] to the excessive amount of computer time that was necessary to carry out the Monte Carlo evaluation of the Wiener integrals encountered in the theory.

Two effects directly influence the curves we have displayed with our data in Figs. 6 and 7. The first is the error associated with the calculated $g(r)$ due to the statistical sampling error involved in the Monte Carlo technique used by Jordan and Fosdick.[10] These errors are implicit in our curves and no attempt has been made to display their effect. The second effect, which gives rise to the spreading or band of $S(k)$ values shown shaded in the figures, is associated with the interpolation and extrapolation of the $g(r)$ values given by Jordan and Fosdick[10] so as to allow a determination of $S(k)$ by Fourier transformation.[33] This effect is a direct result of the limited extent of the available table of values for $W_2(r)$ and $g_1(r)$.

The spreading of possible theoretical $S(k)$ values results primarily from the extrapolation of $g(r)$ (Fig. 8) to unity at large values of r. The complete set of $g(r)$ values at 5 K which one can obtain from the table provided by Jordan[32] is represented in Fig. 8 by the triangular points. Possi-

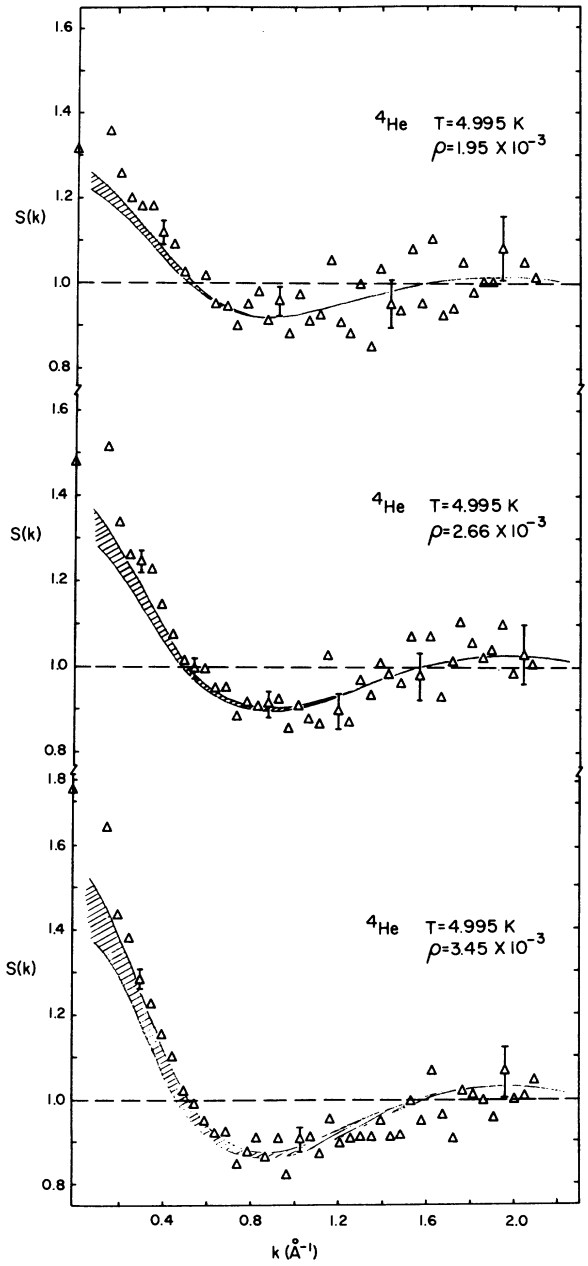

FIG. 7. Structure-factor values for ^{4}He along with the theoretically expected curves. The densities are given in mole/cm^3.

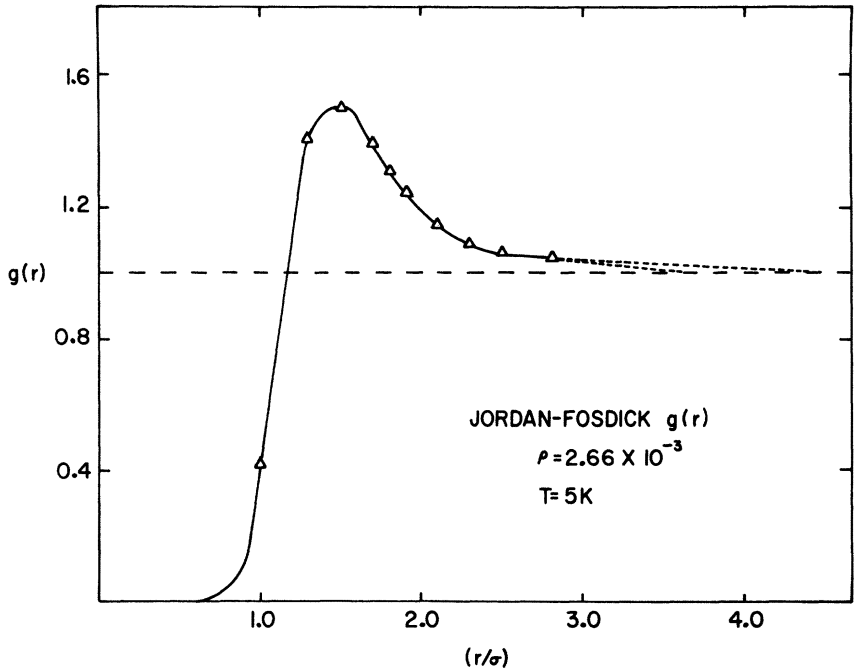

FIG. 8. Pair-correlation function for a density of 2.66×10^{-3} mole/cm^3 in the case of ^{4}He. The result is typical. The triangles are points obtained from $W_2(r)$ and $g_1(r)$ as given by Jordan. To obtain the structure factor $S(k)$ by Fourier transformation one requires modifications: (1) the smooth curve represents interpolation between the points represented by triangles and (2) the dashed line represents the extrapolation to $g(r)=1$ for large values of r. The structure factor for $k\geq0.5$ Å^{-1} obtained is quite insensitive to the details of the interpolation as expected. The spread of $S(k)$ values depicted in Figs. 6 and 7 is a result of the various possible extrapolations we have chosen for each density (and represented here by the dashed lines). Here $\sigma=2.556$ Å.

ble (and admittedly crude) extrapolations to unity are indicated by dashed lines. The two lines shown yield a spreading of $S(k)$ values such as that shown in Fig. 7(b). The effect is largest at higher densities [due to the increased effect of $g_1(r)$ on $g(r)$] as can be seen by reference to Eq. (6) and the plots for $g_1(r)$ given by Jordan and Fosdick.[10] Extrapolations which are more realistic are of course possible and we shall now discuss these as well as various computer fits to the structure factor data in some detail.

It should be emphasized here that we regard our data as being in only *qualitative* agreement with the theory of Jordan and Fosdick. It is clear that since the behavior of $g(r)$ for large r is absent from the theory, the predicted behavior of $S(\vec{k})$ at small $\vec{k}$ can show only fortuitous agreement with experiment. In particular if we denote $S(0)=\rho_0 k_B T X_T$, one possibility for the asymptotic[9] form for $g(r)$ is

$$g(r)=1+\frac{3S(0)[S(0)-1]}{2\pi r r_G^{(2)}\rho}\exp\left[-r\left(\frac{6S(0)}{r_G^{(2)}}\right)^{1/2}\right]. \quad (8)$$

This form bears little resemblance to our straight-line extrapolations. One might hope, perhaps, to modify the Jordan and Fosdick[10] $g(r)$ by applying the above expression at large values of r. Attempts to do this using the experimental $r_G^{(2)}$ values fail because the values of $g(r)$ given by Jordan and Fosdick disagree strongly (50%) with the values given by Eq. (8) in the range of r values where they might be expected to overlap. This disagree-

TABLE I. Values for the moments $r_G^{(2)}$ [Eq. (6)] as determined from power-series fits of the form of Eq. (5) to the data. In each fit, $S(0)=\rho_0 k_B T X_T$ was used as obtained from the virial coefficients (see Appendix A and Table III). $\Delta r_G^{(2)}$ represents a one standard-deviation uncertainty as determined by the fit. The density is given in mole/cm^3 while $r_G^{(2)}$ has units of Å^2.

Sample	Density ($\times10^{-3}$)	r_G^2	Δr_G^2
^{4}He	1.945	9.4	1.0
^{4}He	2.656	20.4	4.0
^{4}He	3.450	45.0	4.0
^{4}He	1.348	7.1	2.3
^{4}He	2.598	24.5	10.0
^{4}He	3.599	52.5	8.0
^{4}He	5.557	193.0	20.0
^{3}He	1.946	10.5	2.0
^{3}He	2.657	16.4	4.0
^{3}He	3.477	27.0	4.0

ment is, however, within the Monte Carlo error estimates for their $g(r)$ values.

As is clear from the shaded curves in Figs. 6 and 7, attempts to obtain the intercept $S(0)$ from the *theoretical* $g(r)$ directly through use of

$$S(0) = 1 + 4\pi\rho \int r^2[g(r) - 1]\, dr \qquad (9)$$

must also fail. We have, as we have indicated, obtained the expected intercept through use of the virial coefficients (Appendix A).

In principle, Eq. (5) can be used to obtain the moments, Eq. (6), of the correlation function by means of an even power series least squares fit to the structure factor data. We have carried out such fits for all of the data presented in the figures. Our errors are such that only meaningful values can be obtained for $r_G^{(2)}$. Values for $r_G^{(4)}$ can also be obtained, but the errors associated with those values are so large as to make the values obtained of limited use. It also should be pointed out that the values obtained for $r_G^{(2)}$ depend somewhat on the range of data and degree of the series used in the fit. In view of this, the values of $r_G^{(2)}$ shown in Table I and Figs. 9 and 10 should be used with caution. In the case of the ^{4}He values we have arbitrarily fit the moments to an equation of the form $r_G^{(2)} = A\rho^B$. Using $r_G^{(2)}$ in Å^2 and ρ in mole/cm^3, we find $A = (5.4 \pm 4.2) \times 10^8$ and $B = 2.87 \pm 0.15$ (three standard-deviation errors). This fit is shown as the straight line on the figure. In Fig. 11 we have plotted $r_G^{(2)}/S(0)$ for ^{4}He as a function of density. Again, a simple power law seems reasonable. The straight line on this figure shows the result of a fit to $r_G^{(2)}/S(0) = C\rho^D$, where we find $C = (1.7 \pm 1.7) \times 10^5$ and $D = 1.96 \pm 0.19$ (again, three standard-deviation errors).

Other two-parameter fits can also be made. For example, we have also fit our data to an expression of the form $r_G^{(2)} = a\rho + b\rho^2$. Using $r_G^{(2)}$ in Å^2 and ρ in mole/cm^3 we find $a = (-1.54 \pm 0.75) \times 10^4$ and $b = (1.07 \pm 0.18) \times 10^7$. This result is unphysical since it suggests that $r_G^{(2)} < 0$ for values of the density below 1×10^{-3} mole/cm^3. As might be expected, three-parameter fits which include a term of order ρ^3 do not suffer from this problem.

We should note here that (5) may not in fact be the best expansion with which to represent the structure factor $S(k)$. In particular, Enderby, Gaskell, and March[34] and also Feenberg[35] have shown that if the interatomic potential falls off at large r as $\phi \sim -A/r^6$, then the structure-factor

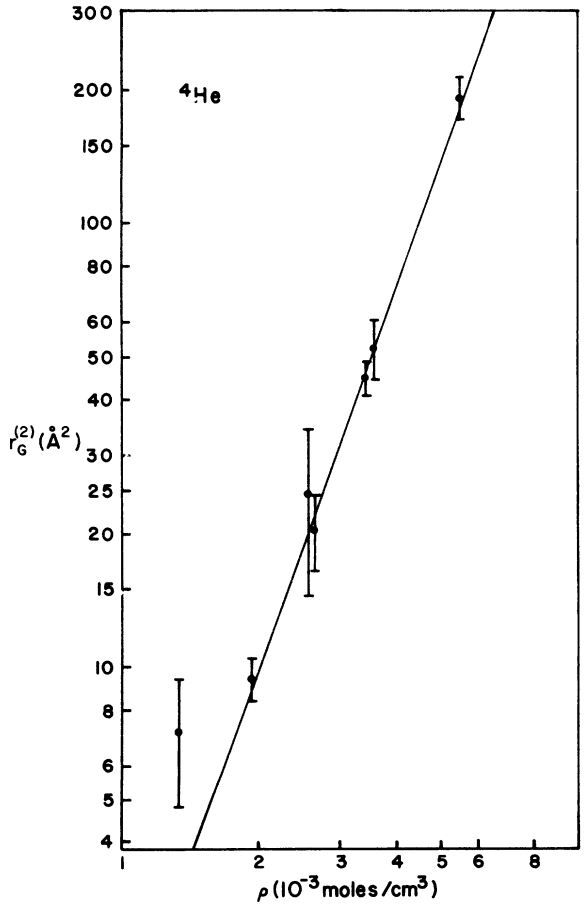

FIG. 9. Moments $r_G^{(2)}$ for ^{4}He. The straight line is a least-squares fit to an expression of the form $r_G^{(2)} = A\rho^B$ as explained in detail in the text.

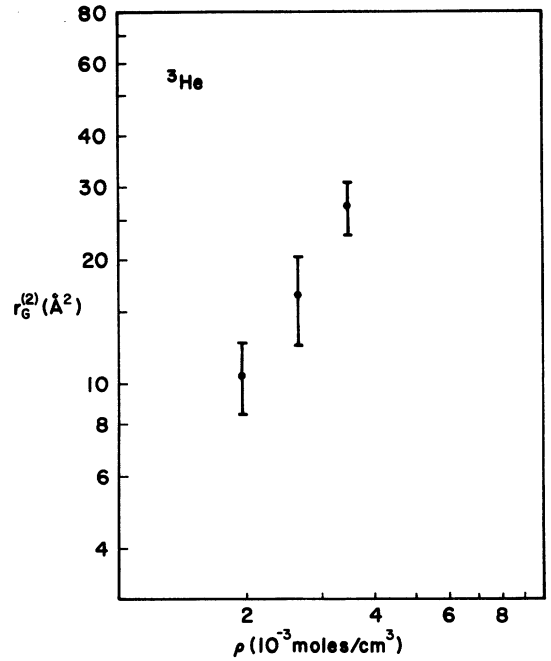

FIG. 10. Moments $r_G^{(2)}$ for ^{3}He. Owing to the limited results for the ^{3}He case, no fit to a power of the density is shown.

expansion should possess a term of order k^3, i.e., we must write

$$S(k) = S(0) + a_2 k^2 + a_3 k^3 \cdots . \tag{10}$$

This differs from Eq. (5) in that it contains odd powers of the momentum transfer. Further, given the presence of a nonzero value for a_3, March[36] and co-workers have shown that the asymptotic form of the pair-correlation function can be expressed as

$$g(r) = 1 + 12a_3/\pi^2 \rho r^6 . \tag{11}$$

Gaskell[37] has shown that within the context of the Born-Green theory one can obtain a specific form for a_3. He writes

$$a_3 = \frac{S(0) A \pi^2 \rho}{12 k_B T} \left(1 - \frac{2(\rho k_B T - p)}{\rho k_B T}\right)^{-1}, \tag{12}$$

where p is the pressure of the gas and A is the strength of the $1/r^6$ term in the interatomic potential. In particular, for a Lennard-Jones potential we have $A = 4\epsilon\sigma^6$, where ϵ is the depth and σ is the characteristic range of the potential. March[36] has pointed out that one should exercise caution in attempting to use Eq. (12), but it does provide us with numbers to which we may compare the results of fits to the $S(k)$ data. We wish to emphasize again at this point that these fits do depend somewhat on the degree of the function and also the range of the data chosen for the fit. We find that fits of the form of

$$S(k) = S(0) + \sum_{n=2}^{m} a_n k^n \tag{13}$$

almost invariably represent our $S(k)$ results better than do fits made by even powers alone [such as Eq. (5)]. The a_2 coefficients of these fits [of the form of Eq. (13)] are presented in Fig. 12. Note that what is actually plotted is the quantity $-6a_2$ which can be compared directly with the $r_G^{(2)}$ values obtained from fits of the form of Eq. (5) which appear in Fig. 9.

These new moments can of course also be fit by expressions of the form $A\rho^B$ and $A\rho + B\rho^2$, etc. Here again we find that better *two-parameter* fits are obtained for functions of the form $r_G^{(2)} = A\rho^B$. In particular, for the ^{4}He case we find (with $r_G^{(2)}$ in Å^2 and ρ in mole/cm^3) $A = (1.40 \pm 2.7) \times 10^8$ and $B = 2.58 \pm 0.36$. Fits of $r_G^{(2)}/S(0)$ values to the form $A\rho^B$ result in the values $A = (9.9 \pm 21) \times 10^5$ and $B = 1.81 \pm 0.39$.

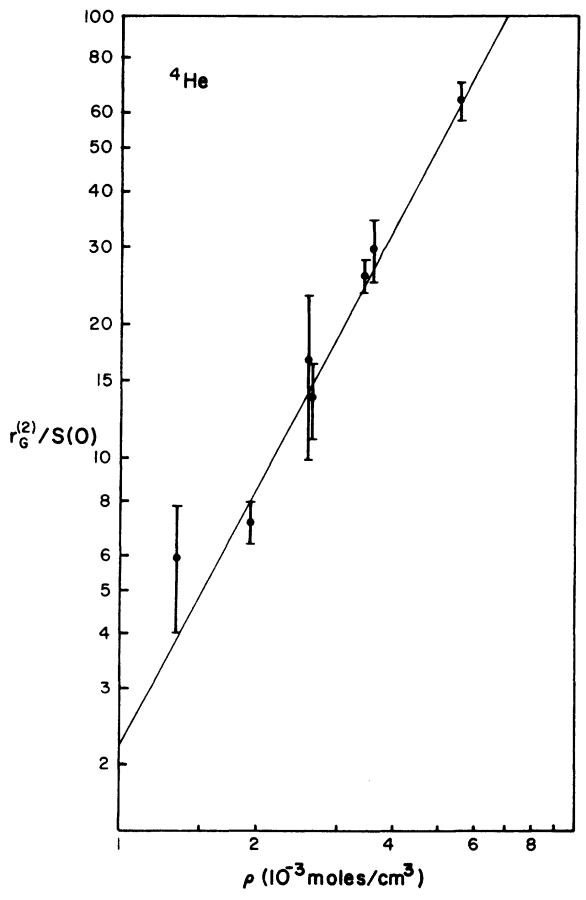

FIG. 11. Quantity $r_G^{(2)}/S(0)$ for ^{4}He as a function of density. The straight line represents the results of a least-squares fit of the form $r_G^{(2)}/S(0) = C\rho^D$ as described in the text.

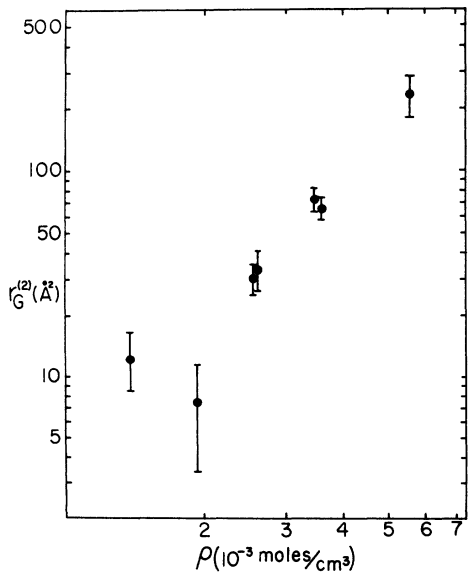

FIG. 12. Coefficients of the k^2 term in fits to the ^{4}He data of the form of Eq. (13). The actual coefficient a_2 is not plotted here. We have plotted the quantity $-6a_2$ which corresponds directly to $r_G^{(2)}$ as displayed in Fig. 9.

TABLE II. The coefficients a_3 as a function of ^{4}He density. Here the density is given in mole/cm^3. The column headed "Theory" gives a_3 values as predicted by Eq. (12). The column headed "Experiment" gives a_3 values determined from fits of the form of Eq. (10) to the $S(k)$ data. These values are averages obtained from several fits of various order applied to various k_m values (where $0 \leq k \leq k_m$). The a_3 coefficients have units Å^3.

Density ($\times 10^{-3}$)	Theory	Experiment
1.348	2.19	5±3
1.945	3.78	3±3
2.598	6.33	12±5
2.656	6.59	9±4
3.450	11.68	23±10
3.599	12.36	25±10
5.557	55.27	110±30

The a_3 coefficients have also been extracted from the fits. These coefficients (shown in Table II) have no analog in Eq. (5). Also shown in Table II are values of a_3 as predicted by Eq. (12). One should make note of the fact that certain fits *can* reproduce the values a_3 as predicted by the theory. We have not selected those particular fits as representative of our data, however, since the fits we have selected give a better χ^2 at smaller values of the momentum transfer than do those which more closely reproduce the predicted a_3 values as given by Eq. (12).

We have attempted to augment the pair correlation function of Jordan and Fosdick by tacking on the asymptotic form represented by Eq. (11). The general shape of the resulting $g(r)$ is displayed in Fig. 13. We have simply made a smooth interpolation between the Jordan-Fosdick values and those given by Eq. (11). It is also possible to invert the interpolated $g(r)$ to obtain a "predicted" $S(k)$. An attempt to do this is shown in Fig. 14. This is typical of the results at other densities. Using the experimentally determined a_3 coefficients in Eq. (11) one can calculate $S(0)$ through use of Eq. (9) and $r_C^{(2)}$ through use of Eq. (6). We find reasonable but by no means perfect agreement with experiment.

Let it suffice to conclude this section with a few comments in summary. We find that expressions of the form of Eq. (10) seem to fit the present data better than do even series expressions of the form of Eq. (5). The resulting coefficients must again be accepted with caution. This is required by the rather large statistical errors in the data and the previously mentioned general dependence of the coefficients on the degree of the polynomial and on the range of the data selected for the fit. We should mention that we have also carried out polynomial weighted least-squares fits of the form

$$S(k) = S(0) + \sum_{n=1}^{m} a_n k^n . \tag{14}$$

We find that these fits, which include *all* powers of the momentum transfer fit the present $S(k)$ data about as well as do fits where terms of order k are absent. Thus, we find $(k^1, k^2, k^3, \ldots)$ fit the

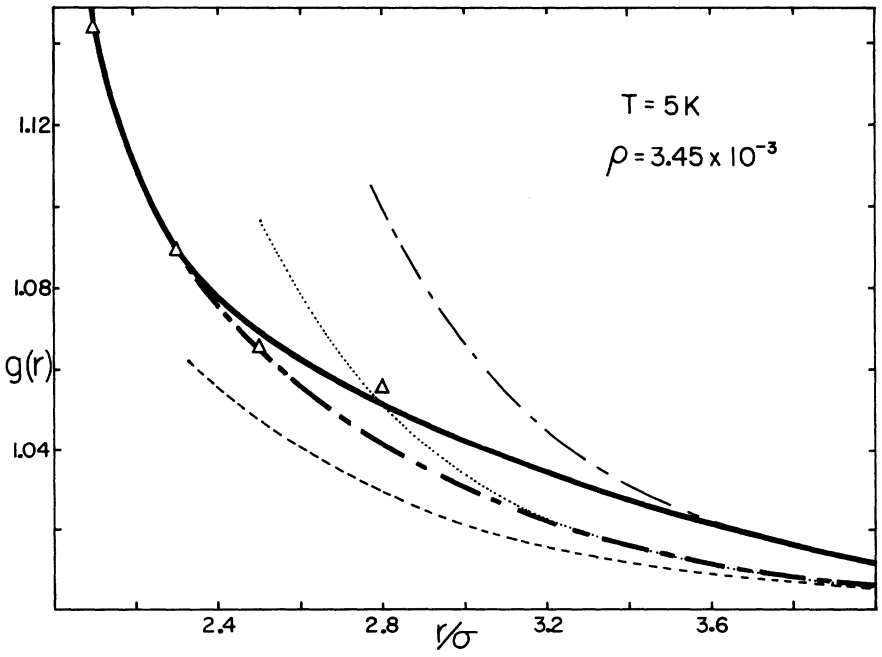

FIG. 13. Various asymptotic tails for the pair-correlation function obtained from the work of Jordan (Ref. 32). The dashed line represents Eq. (8) using $r_C^{(2)}$ as given in Table I. The dotted line represents Eq. (11) using the a_3 value given by Eq. (12). The long-short-dashed line represents Eq. (11) using the experimental value for a_3 given in Table II. The heavy curves represent our interpolations between Jordan's values for $g(r)$ and the values given using Eq. (11) and the various a_3's. Fourier transforms, Eq. (1), of $g(r)$ with the tails represented by the heavy curves are presented in Fig. 14.

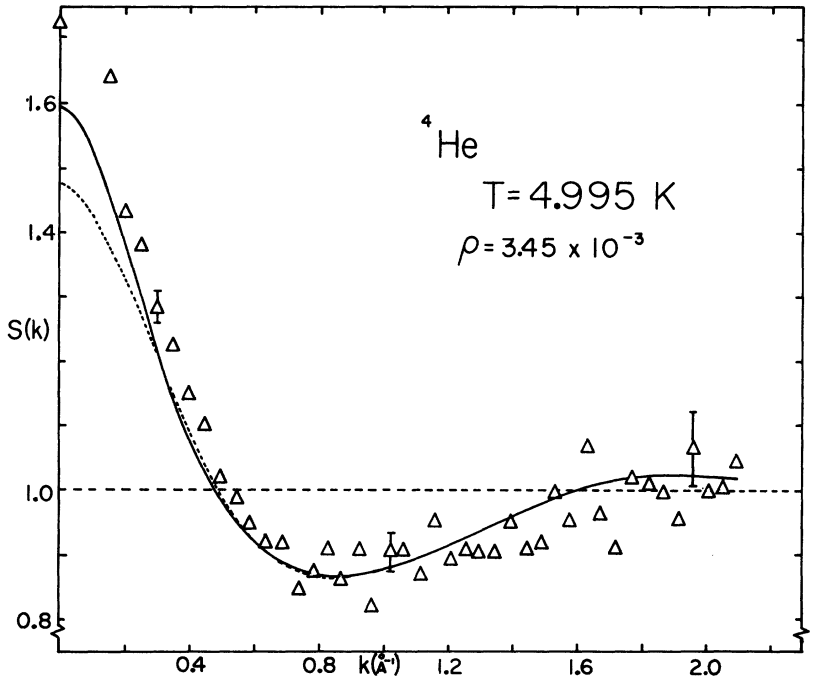

FIG. 14. $S(k)$ vs k for the density $\rho = 3.45\times10^{-3}$ mole/cm^3. Here the curves represent the Fourier transform of the pair-correlation function due to Jordan as modified by interpolation to the asymptotic form Eq. (11). The dashed line represents $S(k)$ obtained using the predicted [Eq. (12)] value of a_3 while the solid line represents the case using the experimental value of a_3 given in Table II. The triangle on the ordinate represents $S(0)$ as obtained from $S(0)=\rho k_B T \chi_T$.

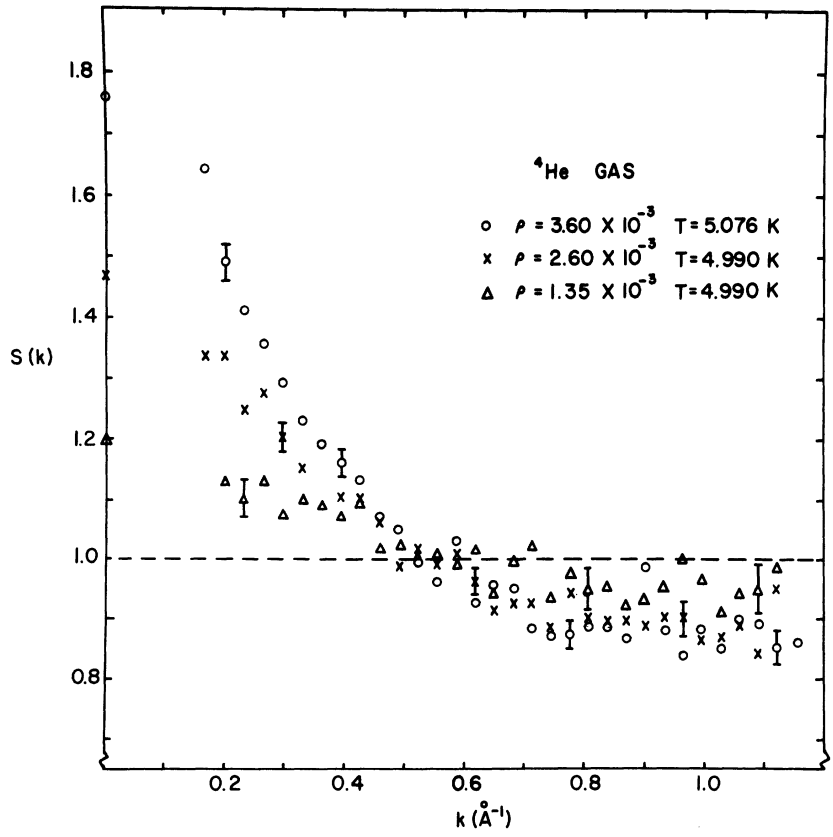

FIG. 15. Small-momentum-transfer results for ^{4}He at several pressures and two temperatures. The density is given in units of mole/cm^3.

data very slightly better than (k^2, k^3, k^4, ...), which in turn fit the data better than fits of the form (k^2, k^4, k^6, ...).

Finally, we must point out that since $g(r)$ represents the conditional probability of finding an helium atom at r given that an helium atom is located at $r=0$ (normalized to unity at $r\to\infty$) it seems unreasonable to expect that $g(r)$ will not exhibit some oscillation beyond $r\approx 3\sigma$. At least one experiment[4] suggests that this will be the case. Thus, our attempts to force an asymptotic tail on the theoretical $g(r)$ due to Jordan are probably premature.

Experiments planned for an apparatus now under construction will be carried out at momentum-transfer values as small as 0.01 Å^{-1} and hence should allow a much better determination of the moments $r_G^{(2)}$. In particular, we expect to be able to test the various expansions for $S(k)$ much more critically with this new apparatus.

In Figs. 15 and 16 we display our more detailed low-momentum-transfer results. Note that the expected zero-momentum-transfer intercept in the case of the data presented in Fig. 16 is 2.99. As one can see, the data do not extend to small enough values of the momentum transfer to cleanly show consistency with this expected intercept.

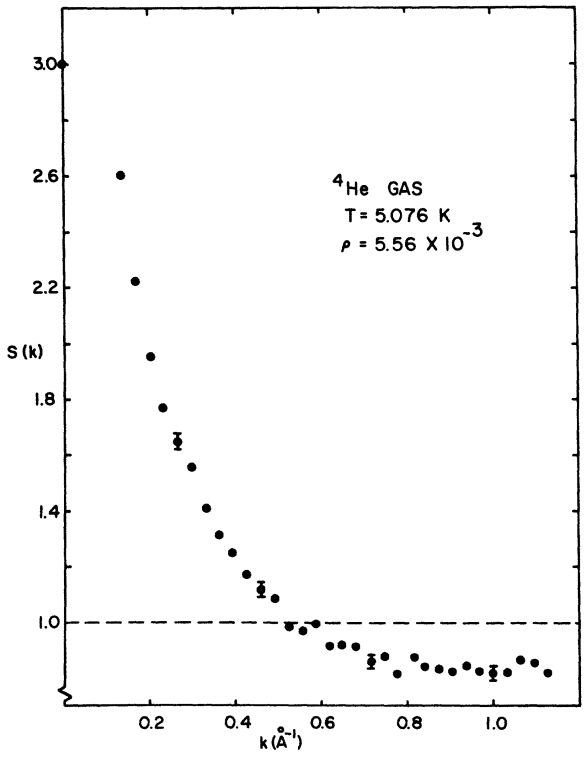

FIG. 16. Small-momentum-transfer results for ^{4}He at the highest density studied: $\rho = 5.56\times 10^{-3}$ mole/cm^3.

Figure 17 displays both gas and liquid data and demonstrates that the behavior exhibited by Fig. 1 is, in fact, what one finds. The structure-factor values for liquid ^{4}He were obtained from the work of Refs. 4 and 19.

VI. CONCLUSIONS

We have reported the first detailed low-momentum-transfer measurements of the structure factor of gaseous ^{3}He and ^{4}He as a function of pressure at several temperatures near 5 K. The observed structure is seen to increase with density as expected. The moments $r_G^{(2)}$ have been measured as a function of density by means of even power-series fits to the structure factor data. Other series expansions have been examined. The theoretical results of Jordan and Fosdick,[10] including various asymptotic modifications are only in qualitative agreement with the experimental results. In particular, our results seem to suggest that the predicted $g(r)$ values are too small at large r. This conclusion must be accepted with caution however since a unified picture of $g(r)$ at intermediate r values does not exist. The existence of these data and the expectation of more detailed results of higher precision in the near future should provide a stimulus for new theoretical efforts in this area.

VII. FUTURE WORK

As we have mentioned, a new x-ray facility is currently under construction. With it we expect to carry out structure factor measurements over

TABLE III. Zero-momentum-transfer structure-factor values for the gases studied in this work. The densities (mole/cm^3) for the various pressure (Torr)-temperature (K) combinations are also given. In the case of neon we see that the structure factor is nearly the same as one would expect for an ideal gas. The values for $S(0)$ can be compared directly with the figures in the main text.

Sample	T	P	ρ	$S(0)$
Neon	77.4	680	1.415×10^{-4}	1.007
^{4}He	4.995	848	3.450×10^{-3}	1.731
	4.995	693	2.656×10^{-3}	1.481
	4.995	534	1.945×10^{-3}	1.312
	5.076	1174	5.557×10^{-3}	2.993
	5.076	894	3.599×10^{-3}	1.758
	4.990	680	2.598×10^{-3}	1.469
	4.990	385	1.348×10^{-3}	1.198
^{3}He	5.230	967	3.477×10^{-3}	1.421
	5.230	767	2.657×10^{-3}	1.302
	5.230	580	1.946×10^{-3}	1.210

the momentum-transfer range $0.01\ \text{Å}^{-1} \leq k \leq 6\ \text{Å}^{-1}$. This new facility will incorporate a high-intensity source and hence result in more precise measurements.

ACKNOWLEDGMENTS

The author is indebted to Professor W. A. Little and the Department of Physics at Stanford University for their warm hospitality while the experimental portion of this work was carried out. He would like to thank L. Goldstein for several interesting and helpful conversations. The author greatfully acknowledges L. Bruch for drawing the work of Refs. 10 and 17 to the attention of the author and also for several very helpful comments on an earlier version of this manuscript. He is indebted to B. L. Weiss for carrying out some of the calculations associated with inverting the pair correlation functions. He would like to thank H. F. Jordan for providing a table of values for $W_2(r)$ and $g_1(r)$ from which the structure factor curves were obtained. He would also like to thank L. Suter for able assistance during a part of the data collection and C. Lyneis for the use of the calibrated germanium-resistance thermometer.

APPENDIX A

In this section we discuss the closeness to ideality of the neon which was used to provide the normalization mentioned in the main text. As we have indicated, the best substance one might use for normalization is a substance whose structure factor is already known. This is true simply because in the comparison between the intensity of scattering from substances A and B,

$$I_A = AN_A T_A(\phi_{Ae} S_A + \phi_{Ai}) \tag{A1}$$

and

$$I_B = AN_B T_B(\phi_{Be} S_B + \phi_{Bi}), \tag{A2}$$

to obtain the structure factor of interest, say S_A, exclusive of geometrical factors

$$S_A = \frac{I_A \rho_B T_B}{I_B \rho_A T_A} \frac{(\phi_{Be} S_B + \phi_{Bi})}{\phi_{Ae}} - \frac{\phi_{Ai}}{\phi_{Ae}}, \tag{A3}$$

one must have prior knowledge of the structure

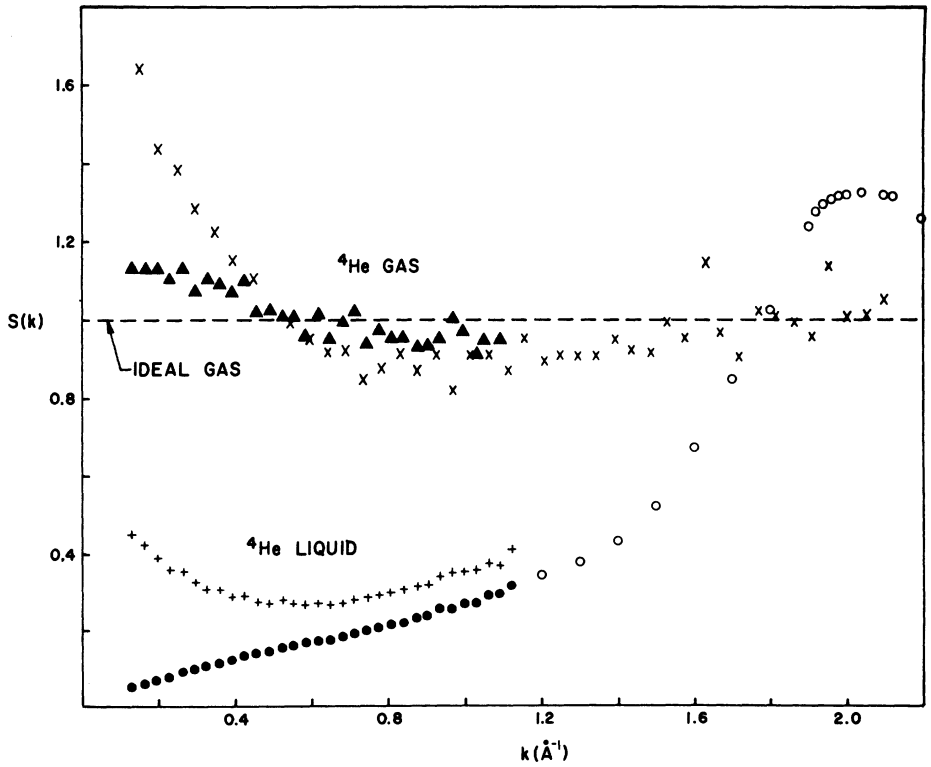

FIG. 17. Composite plot of representative data for ^{4}He in both the gas and liquid phase. The straight-dashed line represents the structure factor of an ideal gas. The symbols represent the structure factor of ^{4}He as follows: ×, gas, $T = 4.99$ K, $\rho = 3.45 \times 10^{-3}$ mole/cm^3; ▲, gas, $T = 4.99$ K, $\rho = 1.35 \times 10^{-3}$ mole/cm^3; ●, liquid, $T = 0.38$ K; +, liquid, $T = 4.60$ K; ○, liquid, $T = 0.79$ K. The data represented by ×, ▲ are from this work; by ●, + from Ref. 19; and by ○ from Ref. 4.

factor S_B. Since this is generally not possible in practice, the next best choice is to pick a substance which is nearly ideal at easily accessible temperatures and pressures. In that case, one simply approximates S_B by unity for all angles of scattering. To make an *accurate* determination of the structure factor of interest S_A, one must make a careful choice for substance B.

The density and other thermodynamic properties of gases are accurately given by the virial coefficients. In particular, one good measure of the departure from ideality of a substance is the value of the quantity $S(k)$ as given by Eq. (5) in the limit of zero momentum transfer $S(0)=\rho_0 k_B T X_T$. For an ideal gas, $X_T=(\rho_0 k_B T)^{-1}$ and $S(0)=1$. Departures from unity represent nonideality and can,

TABLE IV. Structure factor for ^{4}He gas at a temperature of 4.995 K and several pressures. As indicated in the text of this Appendix, $\sigma(\%)$ represents a one standard deviation uncertainty in $S(k)$ expressed as a percent of the $S(k)$ value.

	848 Torr		693 Torr		534 Torr	
k	$S(k)$	$\sigma(\%)$	$S(k)$	$\sigma(\%)$	$S(k)$	$\sigma(\%)$
0.150	1.640	2.10	1.514	2.46	1.357	2.91
0.199	1.435	1.80	1.334	2.12	1.255	2.40
0.248	1.381	1.76	1.262	2.08	1.198	2.33
0.297	1.284	1.80	1.246	2.07	1.179	2.31
0.346	1.226	1.88	1.227	2.13	1.177	2.37
0.394	1.150	1.91	1.140	2.19	1.117	2.41
0.443	1.102	1.98	1.073	2.31	1.089	2.49
0.492	1.023	2.14	1.016	2.48	1.023	2.71
0.541	0.992	2.20	0.997	2.55	0.826	3.22
0.590	0.948	2.29	0.994	2.59	1.016	2.81
0.639	0.919	2.42	0.947	2.78	0.951	3.07
0.687	0.920	2.51	0.954	2.88	0.942	3.23
0.736	0.846	2.63	0.884	3.01	0.900	3.32
0.783	0.875	2.73	0.914	3.12	0.950	3.40
0.830	0.910	2.80	0.903	3.31	0.974	3.51
0.877	0.864	2.87	0.909	3.26	0.911	3.64
0.924	0.908	2.94	0.921	3.41	0.956	3.72
0.970	0.820	3.11	0.850	3.59	0.879	3.94
1.017	0.905	3.11	0.901	3.66	0.971	3.88
1.064	0.904	3.26	0.877	3.92	0.914	4.29
1.110	0.870	3.55	0.865	4.22	0.924	4.55
1.157	0.957	3.55	1.054	3.91	1.054	4.37
1.204	0.897	3.71	0.893	4.39	0.905	4.83
1.250	0.910	3.83	0.868	4.68	0.881	5.26
1.297	0.902	4.08	0.966	4.59	0.997	5.07
1.343	0.906	4.10	0.930	4.76	0.846	5.83
1.390	0.953	4.21	1.002	4.78	1.034	5.28
1.437	0.919	4.45	0.977	5.03	0.949	5.84
1.484	0.916	4.56	0.955	5.23	0.936	6.04
1.532	0.998	4.64	1.073	5.18	1.078	5.83
1.579	0.950	4.84	0.974	5.61	0.950	6.52
1.626	1.143	4.54	1.075	5.48	1.104	6.07
1.673	0.964	5.18	0.925	6.29	0.924	7.20
1.720	0.904	5.30	1.013	5.77	0.938	6.96
1.767	1.024	5.37	1.108	5.94	1.050	6.98
1.814	1.011	5.43	1.053	6.18	0.979	7.42
1.861	0.998	5.26	1.019	6.05	1.000	6.94
1.907	0.958	5.46	1.037	6.06	0.930	7.63
1.954	1.137	5.24	1.095	6.20	1.181	6.58
2.001	1.003	5.61	0.981	6.64	1.586	5.33
2.047	1.005	5.77	1.023	6.65	1.048	7.37
2.094	1.049	5.84	1.002	7.00	1.012	7.84

TABLE V. Structure factor for ^{3}He gas at a temperature of 5.23 K and several pressures.

	967 Torr		767 Torr		580 Torr	
k	$S(k)$	$\sigma(\%)$	$S(k)$	$\sigma(\%)$	$S(k)$	$\sigma(\%)$
0.150	1.336	2.29	1.256	2.74	1.109	3.36
0.199	1.224	1.91	1.207	2.21	1.157	2.49
0.248	1.153	1.90	1.141	2.20	1.065	2.52
0.297	1.141	1.89	1.116	2.19	1.088	2.42
0.346	1.056	2.01	1.079	2.29	1.030	2.59
0.394	1.021	2.01	1.029	2.32	1.047	2.51
0.443	0.975	2.10	1.003	2.40	1.001	2.63
0.492	0.963	2.18	0.972	2.53	0.978	2.77
0.541	0.939	2.24	0.946	2.60	0.952	2.86
0.590	0.903	2.34	0.931	2.69	0.945	2.95
0.639	0.885	2.44	0.907	2.82	0.946	3.05
0.687	0.873	2.56	0.940	2.88	0.937	3.21
0.736	0.867	2.55	0.857	3.03	0.854	3.40
0.783	0.851	2.74	0.894	3.14	0.917	3.45
0.830	0.841	2.89	0.861	3.38	0.896	3.69
0.877	0.852	2.86	0.911	3.23	0.851	3.80
0.924	0.862	2.98	0.925	3.36	0.915	3.79
0.970	0.842	2.99	0.851	3.51	0.890	3.81
1.017	0.863	3.18	0.894	3.66	0.871	4.20
1.064	0.871	3.27	0.893	3.80	0.893	4.28
1.110	0.891	3.44	0.900	4.04	0.901	4.56
1.157	0.957	3.52	0.939	4.20	1.008	4.49
1.204	0.914	3.61	0.975	4.08	0.949	4.69
1.250	0.918	3.78	0.948	4.38	0.935	5.00
1.297	0.937	3.96	0.907	4.78	0.963	5.19
1.343	0.920	4.05	0.865	5.02	0.865	5.74
1.390	0.958	4.21	0.914	5.15	0.880	6.05
1.437	0.906	4.47	0.902	5.32	0.888	6.16
1.484	0.901	4.57	0.946	5.24	0.877	6.35
1.532	1.030	4.54	0.917	5.79	0.945	6.47
1.579	1.026	4.52	1.056	5.20	1.063	5.84
1.626	0.962	5.09	0.886	6.40	0.961	6.90
1.673	0.951	5.16	0.986	5.94	0.981	6.79
1.720	0.988	4.98	0.960	5.99	0.962	6.82
1.767	1.095	5.15	1.030	6.27	1.035	7.11
1.814	1.037	5.32	0.994	6.44	0.985	7.39
1.861	0.924	5.56	0.903	6.69	0.937	7.43
1.907	0.982	5.32	1.018	6.09	0.921	7.44
1.954	1.041	5.53	0.975	6.76	1.026	7.38
2.001	0.983	5.63	0.999	6.52	0.972	7.52
2.047	1.091	5.43	1.021	6.60	1.006	7.53
2.094	0.999	6.00	1.005	6.99	0.978	8.07

as indicated, be computed from the virial coefficients.

In the case of neon, the parameters required can be obtained rather easily from the Berlin[30] virial equation. The Berlin equation is given (for neon) by

$$PV = A + B_p P + C_p P^2 . \quad \text{(A4)}$$

Since the isothermal compressibility is defined by

$$X_T = -\frac{1}{V}\left(\frac{\partial V}{\partial P}\right)_T , \quad \text{(A5)}$$

we have immediately the result that

$$X_T = (1/P)[1 - (1/V)(B_p + 2C_p P)] . \quad \text{(A6)}$$

For this work, the neon was kept at a pressure of 680 ± 1 Torr at a temperature of 77.4 K. These parameters result in a zero-momentum-transfer structure factor of $S_{Ne}(0) = 1.007$. Thus, the substitution of $S = 1$ and the use of neon in place of a perfectly ideal gas results in an error of at most 1%.

The limiting structure factor expected in the cases of helium can also be obtained from the virial coefficients. Following Keller,[31] we write

$$PV = RT + \frac{RT}{V} B_{ii} + \frac{RT}{V^2} C_{ii} , \quad \text{(A7)}$$

where $i = 3$ for ^{3}He and $i = 4$ for ^{4}He. In particular, a satisfactory fit to the thermodynamic data can be obtained if we take

$$B_{44} = (23.05 - 421.17/T), \quad C_{44} = 0; \quad \text{(A8)}$$

TABLE VI. Structure factor for ^{4}He gas at several temperatures and pressures. Longer counting times were used to collect the data which resulted in the values presented in this table. Also, the experimental momentum transfer values are more closely spaced than in Tables IV and V. $S(k)$ values in parentheses have larger errors than those listed (see the text in Appendix B).

	385 Torr 4.99 K		680 Torr 4.99 K		894 Torr 5.076 K		1174 Torr 5.076 K	
k	$S(k)$	σ(%)	$S(k)$	σ(%)	$S(k)$	σ(%)	$S(k)$	σ(%)
0.133	(1.132)	3.38	(1.342)	2.20	(1.825)	2.83	(2.603)	2.68
0.165	(1.132)	2.75	(1.338)	1.87	(1.643)	2.21	(2.221)	2.07
0.198	1.132	2.53	1.337	1.76	1.492	1.95	1.947	1.81
0.230	1.102	2.49	1.251	1.75	1.414	1.92	1.768	1.77
0.263	1.132	2.53	1.277	1.80	1.359	1.87	1.644	1.73
0.295	1.074	2.55	1.207	1.80	1.295	1.88	1.551	1.73
0.328	1.102	2.50	1.151	1.82	1.230	1.93	1.409	1.78
0.360	1.093	2.59	1.197	1.85	1.194	1.94	1.310	1.78
0.392	1.073	2.60	1.106	1.89	1.162	2.00	1.246	1.85
0.425	1.100	2.61	1.103	1.93	1.132	2.01	1.172	1.87
0.457	1.020	2.74	1.064	1.97	1.068	2.07	1.116	1.90
0.490	1.023	2.79	0.989	2.06	1.050	2.25	1.086	2.06
0.522	1.006	2.92	1.016	2.11	0.995	2.15	0.983	1.98
0.554	1.007	2.93	0.996	2.13	0.964	2.21	0.969	2.02
0.586	0.955	3.03	1.010	2.18	1.032	2.36	0.996	2.19
0.618	1.018	3.02	0.961	2.24	0.926	2.35	0.908	2.15
0.649	0.947	3.19	0.914	2.31	0.952	2.41	0.916	2.22
0.681	0.999	3.21	0.926	2.39	0.952	2.48	0.904	2.30
0.713	1.023	3.23	0.925	2.45	0.882	2.45	0.857	2.24
0.745	0.939	3.42	0.880	2.51	0.874	2.59	0.872	2.35
0.777	0.976	3.40	0.944	2.48	0.870	2.68	0.813	2.46
0.808	0.950	3.53	0.903	2.58	0.886	2.78	0.872	2.53
0.840	0.954	3.55	0.891	2.62	0.890	2.81	0.840	2.59
0.872	0.923	3.73	0.895	2.70	0.867	2.89	0.830	2.64
0.904	0.932	3.82	0.886	2.78	0.988	2.85	0.822	2.78
0.935	0.954	3.93	0.903	2.88	0.881	2.99	0.840	2.74
0.967	1.002	3.84	0.901	2.92	0.840	3.11	0.821	2.83
0.999	0.969	3.97	0.864	2.99	0.881	3.13	0.814	2.90
1.031	0.911	4.25	0.870	3.05	0.851	3.28	0.818	3.00
1.062	0.944	4.30	0.892	3.14	0.895	3.38	0.862	3.10
1.094	0.950	4.25	0.840	3.21	0.891	3.39	0.852	3.11
1.125	0.989	4.31	0.950	3.16	0.853	3.45	0.814	3.16

$B_{33} = (4.942 - 270.98/T)$, $C_{33} = 2866/\sqrt{T}$.

The compressibility is given in the general case by

$$X_T = \frac{1}{P}\left(1 + \frac{RT}{PV^2}B_{ii} + \frac{RT}{PV^3}C_{ii}\right)^{-1}. \quad \text{(A9)}$$

The limiting structure factor values for the pressures and temperatures reported in this work are given in Table III.

APPENDIX B

This Appendix contains tables of structure-factor values Tables IV–VI determined in the measurements we have reported here. In each case the value given for $S(k)$ has been determined directly from Eq. (4)—the data have not been smoothed in any way. The column headed by $\sigma(\%)$ represents a one standard-deviation uncertainty in $S(k)$ due to counting statistics alone and is expressed as a percent of the given structure factor value. Values of the momentum transfer k are expressed in Å^{-1}. The pressures listed are the experimental gas pressures at the indicated temperatures. The corresponding density for a given pressure-temperature combination can be found by reference to Table III. At the smallest scattering angles very slight misalignments of the spectrometer result in rather large errors in a determination of $S(k)$ due to the steeply rising scattering contribution from the target cell walls. Values of $S(k)$ for momentum transfer values $k \lesssim 0.2$ Å^{-1} should thus be accepted with caution.

---

*Supported in part by the National Science Foundation, the Advanced Research Projects Agency through the Center for Materials Research at Stanford University and by the University Computation Center at the University of Massachusetts at Amherst.

†Work partially carried out while the author was under the tenure of an AFOSR-NRC Postdoctoral Award.

‡Alfred P. Sloan Fellow.

[1]See, for example, A. H. Compton and S. K. Allison, *X-Rays in Theory and Experiment* (Van Nostrand, New York, 1935); H. P. Klug and L. E. Alexander, *X-Ray Diffraction Procedures* (Wiley, New York, 1954); E. F. Kaelble, *Handbook of X-Rays* (McGraw-Hill, New York, 1967).

[2]See, for example, P. A. Egelstaff, *An Introduction to the Liquid State* (Academic, London, 1967); M. S. Green, *The Molecular Theory of Fluids* (North-Holland, Amsterdam, 1952).

[3]See, for example, N. S. Gingrich, Rev. Mod. Phys. **15**, 90 (1943); and Refs. 7 and 19.

[4]E. K. Achter and L. Meyer, Phys. Rev. **188**, 291 (1969).

[5]R. B. Hallock, Phys. Rev. Lett. **23**, 830 (1969); and Ph.D. dissertation (Stanford University, 1969) (unpublished) (available from University Microfilms, Ann Arbor, Mich).

[6]W. L. Gordon (private communication).

[7]W. L. Gordon, C. H. Shaw, and J. G. Daunt, J. Phys. Chem. Solids **5**, 117 (1958).

[8]The spectrometer used in this work was designed primarily to examine the structure factor of ^{4}He liquid at momentum transfer values below 1.1 Å^{-1}.

[9]L. Goldstein, Phys. Rev. **84**, 466 (1951).

[10]H. F. Jordan and L. D. Fosdick, Phys. Rev. **171**, 128 (1968).

[11]W. E. Massey, Phys. Rev. **151**, 153 (1966).

[12]The literature relating to the structure factor of liquids (and in particular quantum liquids) is quite extensive. For a general discussion of structure in the quantum liquids (both theory and experiment) see R. B. Hallock (unpublished).

[13]S. Y. Larsen, K. Witte, and J. E. Kilpatrick, J. Chem. Phys. **44**, 213 (1966).

[14]See, for example, E. Feenberg, *Theory of Quantum Fluids* (Academic, New York, 1969).

[15]T. D. Lee and C. N. Yang, Phys. Rev. **113**, 1165 (1959).

[16]See, for example, A. Ralston, *A First Course in Numerical Analysis* (McGraw-Hill, New York, 1965).

[17]L. D. Fosdick and H. F. Jordan, Phys. Rev. **143**, 58 (1966).

[18]See, for example, M. Kac, *Lectures in Applied Mathematics, Proceedings of the Summer Seminar, Boulder, Colorado, 1957* (Interscience, New York, 1958), Vol. 1.

[19]R. B. Hallock, Phys. Rev. A **5**, 320 (1972).

[20]R. B. Hallock, J. Low Temp. Phys. **9**, 109 (1972).

[21]R. B. Hallock, Rev. Sci. Instrum. **41**, 1107 (1970).

[22]Cryocal germanium thermometer, calibrated from 1 to 10 K, available from Cryocal Corp.

[23]Apiezon *N* grease is available from the James Biddle Co.

[24]Earlier work, see Ref. 5, indicated that our statistical errors due to counting statistics alone would be of the order of 5%. Errors of this magnitude make temperature regulation in excess of a few millikelvin frivolous.

[25]Available from Reuter Stokes, Cleveland, Ohio. The output from the RSG-81 was resolved into two components on a PDP-9.

[26]See, for example, I. A. Blech and B. L. Averbach, Phys. Rev. **131**, A113 (1965), and G. H. Vineyard, Phys. Rev. **96**, 93 (1954).

[27]Y. K. Kim and M. Inokuti, Phys. Rev. **165**, 39 (1967).

[28]C. Tovard, D. Nocholas, and M. Rovault, J. Chim. Phys. **64**, 540 (1967).

[29]*International Table for X-Ray Crystallography*, edited by K. Lonsdale (Kynoch, Birmingham, England, 1962), Vol. III.

[30]*Argon, Helium and the Rare Gases*, edited by G. A. Cook (Interscience, New York, 1961), p. 262.

[31]W. E. Keller, *Helium 3 and Helium 4* (Plenum, New York, 1969).

[32]H. F. Jordan, Ph.D. dissertation (University of Illinois, 1968) (unpublished).

[33]Since the pair-correlation function is only dependent on the separation between atoms, the Fourier integral reduces to the simple form $S(k) = 1 + 4\pi\rho\int[\sin(kr)/kr][g(r) - 1]\, r^2 dr$.

[34]J. E. Enderby, T. Gaskell, and N. H. March, Proc. Phys. Soc. Lond. **85**, 217 (1965).

[35]E. Feenberg, Phys. Rev. Lett. **26**, 301 (1971).

[36]N. H. March, *Scottish Universities Summer School*, 8th, edited by R. C. Clark and G. H. Derrick (Plenum, New York, 1968), p. 348.

[37]T. Gaskell, Proc. Phys. Soc. Lond. **86**, 693 (1965).